

Two-phonon pseudogap in the Klein-Gordon lattice

LAURENT PROVILLE

*Service de Recherches de Métallurgie Physique, CEA-Saclay/DEN/DMN
91191-Gif-sur-Yvette Cedex, France*

PACS. 63.20.Ry – Anharmonic lattice modes.

PACS. 03.65.Ge – Solutions of wave equations: bound states.

PACS. 11.10.Lm – Nonlinear or nonlocal theories and models.

Abstract. – The energy spectrum of the quantum Klein-Gordon (KG) lattice is computed numerically for model parameters relevant to optical phonon spectra. A pairing of phonon states is found when nonlinearity is significant, which agrees with other studies on different quantum lattice models [1, 2]. It results from the lattice anharmonicity, the magnitude of which is quantified by the binding energy of phonon bound states. Our work focuses on the case of weak anharmonicity, i.e., the phonon binding energy is weaker than the single phonon band width. We find that the phonon pairs dissociate at the center of the lattice Brillouin zone, whereas at the edge the binding energy remains comparable to the width of the single phonon band. Consequently, a weak nonlinearity is characterized by a pseudogap in the energy spectrum of two-phonon states.

The phonon frequencies are some fundamental quantities that provide information about atomic interactions and local structure in crystals as well as in polymers or proteins. At the atomic scale, the phonon frequencies are formally derived from the quadratic expansion of the potential energy with respect to atomic displacements. Actually a more accurate description of the potential energy might be obtained by a higher order expansion which involves some non-quadratic terms. Those terms are usually referred to as nonlinear terms because they yield some forces that are not proportional to displacements. In the early seventies, the non-quadratic contribution to the energy has been quantified in molecular crystals such as CO_2 , N_2O and OCS (see Ref. [3] and Refs. therein). The nonlinearity was then identified by some anharmonic peaks in the infrared spectrum. In solid H_2 , similar infrared resonances were earlier interpreted [4] as a signature of phonons pairing. Currently the list of materials in which phonon bound states occur is still growing [5, 6]. In addition, some controversial cases, as for instance acetanilide [7] or the spectral branch $\Delta'_2(LO)$ of diamond [8, 9] can be mentioned as still open questions. In the present study, we point out a possible difficulty for the vibration spectrum interpretation which could occur when nonlinearity is not sufficiently strong to separate the anharmonic resonances from the harmonic energy regions. Then, the hybridization between bound and unbound phonons is shown to imply a pseudogap in the lattice energy spectrum.

The anharmonicity of molecular crystals has been theoretically studied by V.M. Agranovich [1], who proposed a qualitative approach where some boson quasi-particles model the

atom vibrations. A Hubbard onsite interaction between boson pairs was introduced to simulate the nonlinear behavior of the lattice (for recent studies see Ref. [2, 10]). This effective boson model displayed the concepts of phonon bound states and more specifically of biphonon. The drawback of the model is that the energy terms that do not conserve the boson number are neglected, although those terms stem from the potential energy of atoms (or molecules). A rigorous approach to models which do not have a conserved boson number was proposed in Ref. [11]. The present paper can be considered as numerical support for that theory. Here, a numerical method is introduced for computing the KG energy spectrum with different forms of nonlinearity, i.e., different orders in the potential energy expansion. Our technique is based on the construction of a nonlinear phonon basis which allows to treat lattices whatever the magnitude of nonlinearity is, in contrast to the linear phonon basis [12], derived from the harmonic approximation. The attractive advantage of our method is that the maximum size of the lattices that can be studied is large enough to approach the infinite system features, i.e., the energy spectrum shows no boundary effects and it is nearly continuous in the reciprocal space.

The KG model may be introduced as follows. At the node i of a translational invariant d -dimensional lattice, the internal mode x_i of a unit cell (a molecule, for instance) evolves in the local potential V with an effective mass m , each of the x_i being coupled to the nearest neighbors' modes by a quadratic coupling, parametrized by c . Then, the Hamiltonian of that system reads:

$$H = \sum_i \left[\frac{p_i^2}{2m} + V(x_i) - c \sum_{j=<i>} (x_i - x_j)^2 \right]. \quad (1)$$

The subscript $j = < i >$ denotes the first neighbors of site i . The operator x_i and its conjugate momentum p_i satisfy $[x_i, p_i] = i\hbar$. For small amplitudes of x_i , the Taylor expansion of V gives $V(x_i) = a_2 x_i^2 + a_3 x_i^3 + a_4 x_i^4$. It has been limited to the fourth order but higher order terms can be taken into account with no difficulties in calculations that follow. Higher order coupling terms have been found not to modify qualitatively our results. Introducing the dimensionless coefficients and operators:

$$\begin{aligned} A_3 &= a_3 \sqrt{\frac{\hbar}{m^3 \Omega^5}}, \quad A_4 = a_4 \frac{\hbar}{m^2 \Omega^3}, \quad C = \frac{4c}{m \Omega^2} \\ P_i &= p_i / \sqrt{m \hbar \Omega} \quad \text{and} \quad X_i = x_i \sqrt{m \Omega / \hbar} \end{aligned} \quad (2)$$

where the frequency $\Omega = \sqrt{2(a_2 - (2d)c)/m}$ characterizes the d -dimensional oscillator networks, the Hamiltonian reads:

$$H = \hbar \Omega \sum_i \left[\frac{P_i^2}{2} + \frac{X_i^2}{2} + A_3 X_i^3 + A_4 X_i^4 + \frac{C}{2} X_i \sum_{j=<i>} X_j \right]. \quad (3)$$

Note that the coupling coefficient c contributes to Ω . The width of an optical phonon band is physically a few percent of the elementary excitation energy ($\approx \hbar \Omega$). We restrict our study to $A_4 \geq 0$ to ensure that the local potential V is positive when the onsite displacement increases arbitrarily. In contrast, A_3 can take positive or negative values provided V is a monotonic function.

Our computation is now described. The first step is to calculate eigenstates of the onsite Hamiltonian $h_i = P_i^2/2 + X_i^2/2 + A_3 X_i^3 + A_4 X_i^4$, which is performed by projecting h_i over the usual Einstein basis. The diagonalization of the corresponding matrix is realized numerically with great accuracy. The eigenstates of h_i are arranged by increasing order of eigenvalues,

so the α^{th} eigenstate is denoted $\phi_{\alpha,i}$ and its eigenvalue is $\gamma(\alpha)$. Considering the Hamiltonian $H_0 = \hbar\Omega \sum_i h_i$, the H_0 eigenstates can be written as products of onsite states $\Pi_i \phi_{\alpha_i,i}$. Taking advantage of the lattice translational degeneracy, some Bloch waves are constructed from those products as follows:

$$B_{[\Pi_i \alpha_i]}(q) = \frac{1}{\sqrt{A_{[\Pi_i \alpha_i]}}} \sum_j e^{-iq \times j a_0} \Pi_i \phi_{\alpha_i,i-j} \quad (4)$$

where a_0 is the lattice parameter, q is the wave vector, the subscript $[\Pi_i \alpha_i]$ identifies different types of products and $A_{[\Pi_i \alpha_i]}$ ensures the normalization. Expanding the Hamiltonian H in the Bloch waves is done analytically and gives a matrix $\mathcal{B}(q)$. Since H does not hybridize Bloch waves with different q , the diagonalization of $\mathcal{B}(q)$ can be performed independently for each q . To that aim, we used exact numerical methods (LAPACK or Numerical Recipes) on a simple desktop PC. Then, the Schrödinger equation is solved with an error which shrinks to zero exponentially by increasing the cutoff over the H_0 eigenstates. The cutoff is fixed by $\sum_i \alpha_i < N_{cut}$. The number of Bloch waves involved in diagonalization is 3052 for a lattice size $S = 33$. The accuracy of our calculations has been tested both on the anharmonic atomic chain $S = 4$ [12] and the harmonic chain for which the eigenvalue problem is solved analytically by a spatial Fourier transform of Eq. 1. For these two comparisons, very good agreements have been found. For the latter case, the results are reported in Fig. 1. Some distinct cutoff values N_{cut} have been tested and clearly our eigenvalue evaluation converges to the exact values as the cutoff increases. For two-phonon excitations, the error is less than 0.1% when $N_{cut} = 4$. Then the accuracy is even better for the phonon band which fits the dispersion law: $\hbar\Omega\sqrt{1 + 2C \cos(qa_0)}$.

Our results are first presented for a 1D lattice. In Figs. 2(a-c), for a finite size $S = 33$, the eigen-energies (circle symbols) are plotted versus the wave momentum q . They contribute to the distinct branches of the spectrum. When the non-quadratic part of the energy is negligible, the eigen-spectrum is composed of the fundamental optical branch and the linear superpositions of phonon states. Increasing gradually A_4 , fixing $C = 0.05$ (relevant for optical phonons, see Fig. 2(a)) and $A_3 = 0$, makes a branch split from the top of the two-phonon band. Then, the onsite potential V is said to harden. Subsequently, if A_4 is fixed to a positive arbitrary value and A_3 is increased in absolute value, the isolated branch backs into the two-phonon band and eventually splits from the bottom for large enough $|A_3|$. The onsite potential V is now said to soften. By analogy with the biphonon theory [1], the splitting branch (labelled by $\{2\}$ in Figs. 2(b-c)) is identified as being the energy of biphonon states. Measuring the energy of the biphonon with reference to the unbound two-phonon states for same momentum q , a biphonon binding energy can be defined. The absolute value minimum, with respect to q of the biphonon binding energy is called the biphonon energy gap. When the non-quadratic contribution is not sufficient to open the biphonon gap, the gap is found to close at the center of the lattice Brillouin zone (BZ) (Fig. 2(c)). On the other hand, at the edge of BZ the binding energy may remain comparable to the width of the single phonon branch. Thus, a pseudogap occurs when the non-quadratic energy has the same magnitude as inter-site coupling. Similar pseudogaps have been found in other quantum lattices [13, 14]. In the pseudogap regime, biphonon excitations exist only at the edge of BZ while they dissociate into unbound phonon pairs at center of the zone. In Figs. 2(b-c), it is noteworthy that the hybridization between the biphonon states and the two-phonon states modifies substantially the biphonon branch curvature and consequently the quantum mobility of the biphonon. Such a feature can not be analyzed accurately within the effective Hubbard model for bosons since it neglects some energy terms that do not conserve the boson number. The same remark holds for the single

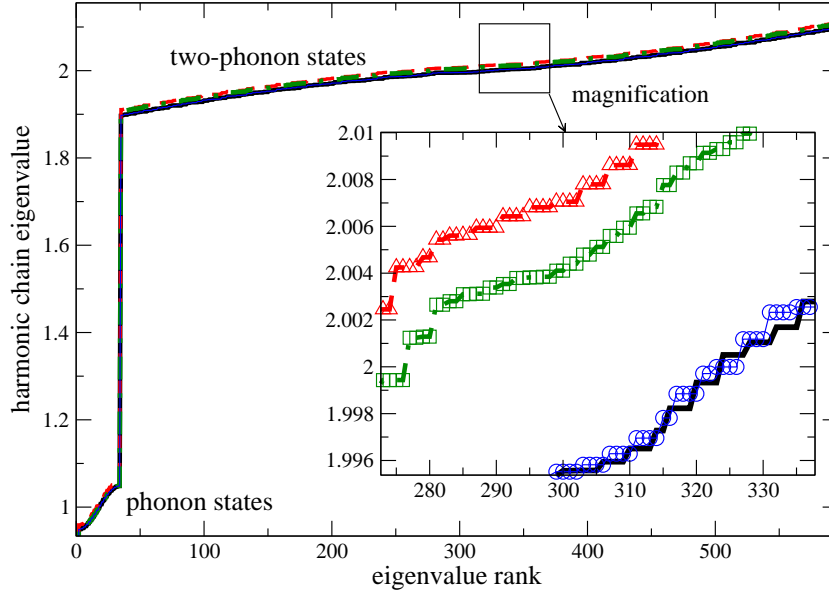


Fig. 1 – For a dimensionless coupling $C = 0.05$, comparison between the exact calculation (thick solid line) and our evaluations (detailed in the text) of the eigenvalues in a 1D harmonic lattice composed of $S = 33$ oscillators. Our numerics are performed for 3 distinct cutoffs $N_{cut} = 2$ (dashed line, triangles), $N_{cut} = 3$ (dot-dashed line, squares) and $N_{cut} = 4$ (thin solid line, circles). The spectrum is measured with respect to the groundstate and is arranged in increasing order. The eigenstate number is reported on the X-axis. The Y-axis unit is $\hbar\Omega$.

phonon dispersion law which takes the form $(1 + C\cos(qa_0))$ (with arbitrary energy units) in the effective boson model instead of the well-known $\sqrt{1 + 2C\cos(qa_0)}$, calculated in the harmonic approximation for similar parameters. The two formulas diverge with increasing C , i.e. when the quantum hybridization is amplified. This disagreement is due to the boson product operators such as $(a_{i+1}^+ a_i^+)$ that are neglected in the effective boson model, in contrast to the KG model and its harmonic approximation.

Other computations have been performed with different model parameters to complete our results. The curvature of the biphonon branch depends on the sign of C provided the biphonon gap is large. Otherwise, the hybridization between bound and unbound phonons tends to impose the same curvature as the two-phonon band (Fig. 2(c)). The biphonon band curvature thus results from the interplay between the biphonon tunneling and the hybridization with unbound phonons. In Fig. 2(b), the triphonon energy branch (labelled by $\{3\}$) which splits from the three-phonon band (not plotted) can also be noted with a similar behavior as the biphonon branch. For the same nonlinear coefficients as in Figs. 2(a-b), varying artificially C to the trivial case $C = 0$ (see Fig. 3) demonstrates that the isolated branches, $\{1\}$, $\{2\}$ and $\{3\}$ coincide with the energies of Bloch waves $B_{[\alpha,0,...]}$ with a single onsite excitation $\alpha = 1, 2$ and 3 , respectively. The branch tag corresponds to the excitation level $\{\alpha\}$ of the coinciding Bloch waves at $C = 0$. The reason for the isolated branches is the anharmonicity of h_i eigenvalues $\gamma(\alpha > 1)$ which implies some energy gaps at $C = 0$ that persist when $C \neq 0$. In Fig. 3, we note the bands associated to unbound phonon pairs, to unbound three-phonon states and to unbound states composed of a biphonon and a single phonon. These states are labelled by multiple tags $\{\alpha, \beta, \dots\}$ that correspond to Bloch waves $B_{[\alpha, \dots, \beta, \dots]}$ at $C = 0$.

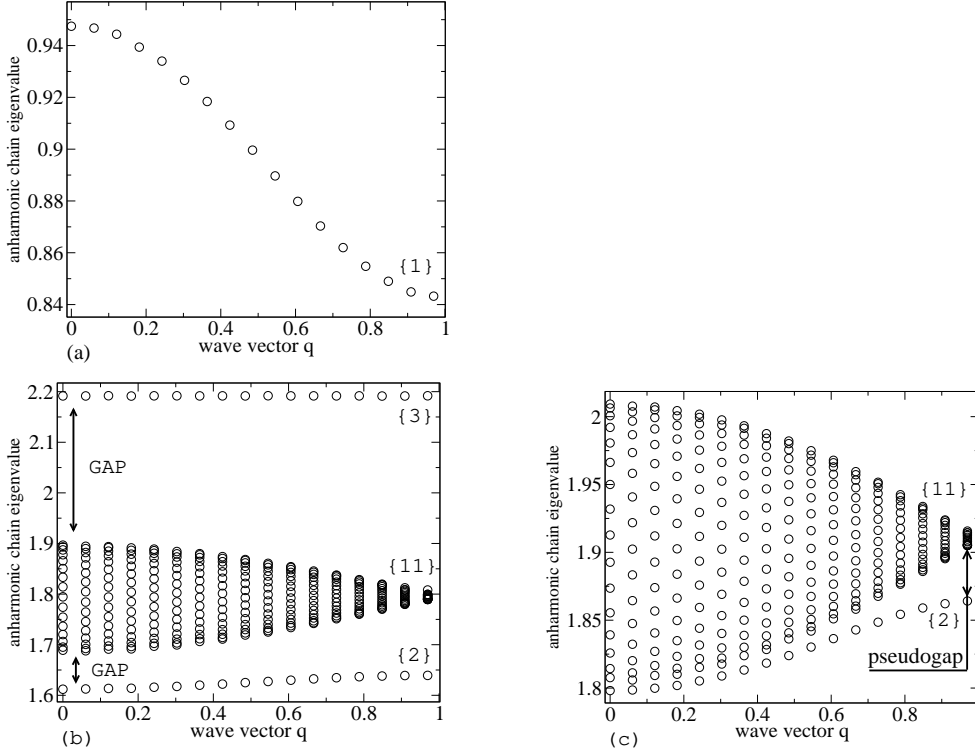


Fig. 2 – Energy spectrum of a chain composed of $S = 33$ unit cells: (a) the optical phonon branch for model parameters $C = 0.05$, $A_3 = 0.13$ and $A_4 = 0.01$; (b) the two-phonon energy region for same parameters as (a); (c) same as (b) but $A_3 = 0.1$. The biphonon branch is labelled by $\{2\}$, the unbound two-phonon bands by $\{11\}$ and the triphonon branch by $\{3\}$. The Y-axis unit is $\hbar\Omega$ and its zero is groundstate energy. The wave vector q is reported on the X-axis, whose unit is (π/a_0) . It ranges from the center to the edge of the first lattice Brillouin zone.

Since our calculations are performed with large enough lattices to avoid boundary effects, there is a perfect agreement between the energy spectrum computed with $S = 33$ (Fig. 2(a-b)) and with $S = 19$ (Fig. 3) for the same parameters. In Fig. 3, the band widths of phonon bound states increase with C much slower than for unbound phonons. The branches of biphonon $\{\alpha = 2\}$ and triphonon $\{\alpha = 3\}$ are found to merge with the unbound phonon bands above a certain threshold C_α . For $C < C_\alpha$, the α^{th} branch is separated from the rest of the spectrum by gaps that open over the whole BZ whereas around $C \approx C_\alpha$, only a pseudogap separates partially that branch from a certain unbound phonon band. The C_α threshold depends on both A_3 and A_4 and it is different for each phonon bound state. When C is much larger than C_2 , the biphonon gap is closed then only gaps of high order phonon bound states (such as triphonon) may be opened in the excitation spectrum. The results reported in Fig. 3 are qualitatively similar to the Raman analysis [15] of the high pressure molecular solid H_2 which shows a pressure-induced bound-unbound transition of the so called bivibron, around 25 GPa (compare Fig.10 in Ref. [15] and the two-phonon energy region in Fig. 3). In the framework of our model, the pressure variation of experiments [15] can be simulated by a change of coupling integral C due to the fact that neighboring molecules are moved closer together because of the external pressure. The increase of C induces a bound-unbound transition of the biphonon

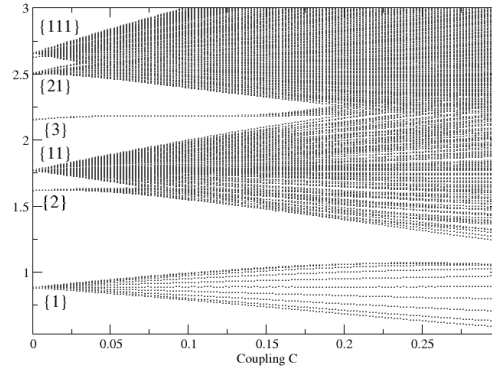


Fig. 3 – Plot of the energy spectrum versus dimensionless coupling C , for a 1D quantum chain composed of $S = 19$ cells with model parameters $A_3 = 0.13$ and $A_4 = 0.01$. The energy unit is same as in Fig. 2. Labels are explained in the text.

at $C = C_2$. The pressure variation of C as well as of other KG model parameters could inform us on how atomic potentials depend on the inter-atomic distances (that are known from diffraction measures). A biphonon is also exhibited by the internal stretching [5] of CO molecules adsorbed on the surface $Ru(111)$. There, the coverage of the surface can also be thought to change the coupling integral C , and a bound-unbound transition could thus be expected at high surface coverage. Yet, that assumption is seemingly inapplicable according to a recent theoretical work [10] which invoked a *coverage dependant anharmonicity* which would originate in a chemical modification of the intramolecular CO potential due to surrounding molecules.

Finally, for a 2D lattice, a biphonon pseudogap is found to open around $q = 1/2$ [11] (see Fig. 4). As we chose a set of nonlinear parameters such that the local potential V hardens, the biphonon energy is higher than for two-phonon instead of lower when V softens (see Fig. 2). Aside from that point, the binding energy vanishes at center of BZ whereas the width of pseudogap at the edge of BZ has same order as the phonon branch width. That likeness between 1D and 2D spectra shows that the pseudogap is a consistent property of lattices where nonlinearity is comparable to the inter-site coupling, whatever the dimensions are. For a 3D lattice, the biphonon pseudogap is expected to open around $q = 1/2$ [11].

To summarize, the energy spectrum of the KG lattice has been considered with numerics. The KG Hamiltonian provides a realistic modelling of both quantum hybridization and pairing of phonon states. Through our computing method, the spectral features of phonon bound states can be related unambiguously to non-quadratic terms of the potential energy. We predict that when those terms are not strong enough to separate the spectral resonances of bound and unbound phonon states, the pseudogaps of the biphonon, triphonon or even higher order of phonon bound states, are potential signatures of nonlinearity. The biphonon pseudogap has been proved to open systematically at the edge of the first Brillouin zone.

* * *

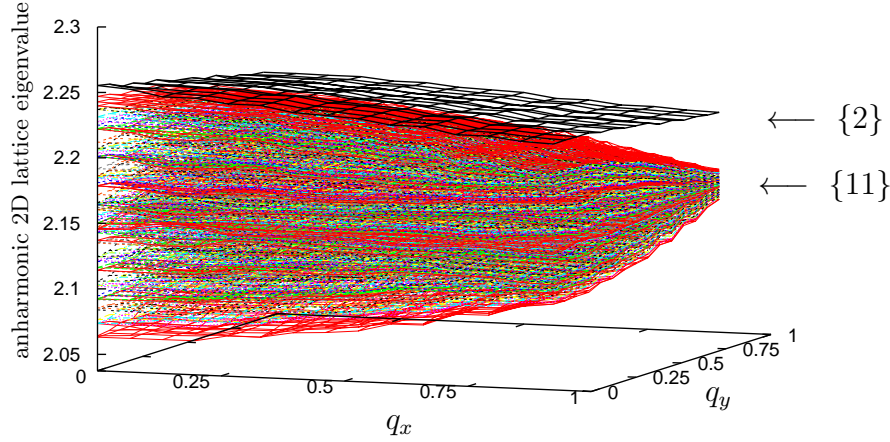


Fig. 4 – Two-phonon spectrum for a 2D square lattice composed of $S = 13 \times 13$ cells and for the model parameters $C = 0.025$, $A_3 = 0$ and $A_4 = 0.025$. Energy unit and tags are same as in Fig. 2. The color picture (easier to read) is available online.

I gratefully acknowledge financial support from Trinity College and an EC network grant on “Statistical Physics and Dynamics of Extended Systems”. Many thanks are addressed to Robert S. MacKay and Serge Aubry.

REFERENCES

- [1] V.M. AGRANOVICH, *Spectroscopy and excitation dynamics of condensed molecular systems*, edited by V.M. AGRANOVICH and R. M. HOCHSTRASSER (North-Holland publishing company)1983, pp. 83-138-.
- [2] J. C. EILBECK, *Proceedings of the Third Conference Localization and Energy Transfer in Non-linear Systems*, edited by L. VAZQUEZ, R. S. MACKAY, M. P. ZORZANO (World Scientific Singapore)2003, p. 177.
- [3] F. BOGANI, *J. Phys. C: Solid State Phys.*, **11** (1978) 1283; **11** (1978) 1297.
- [4] M.P. GUSH, W.F. HARE, E.J. ALLIN AND H.C. WELSH, *Phys. Rev.*, **106** (1957) 1101.
- [5] P. JAKOB, *Phys. Rev. Lett.*, **77** (1996) 4229.
- [6] B.I. SWANSON *et al.*, *Phys. Rev. Lett.*, **82** (1999) 3288.
- [7] J. ELDER and P. HAMM, *J. Chem. Phys.*, **119** (2003) 2709.
- [8] MORREL H. COHEN AND J. RUVALDS, *Phys. Rev. Lett.*, **23** (1969) 1378.
- [9] R. TUBINO AND J. L. BIRMAN, *Phys. Rev. Lett.*, **35** (1975) 670.
- [10] V. POUTHIER, *J. Chem. Phys.*, **118** (2003) 9364.
- [11] R.S. MACKAY, *Physica A*, **288** (2000) 174.
- [12] W.Z. WANG *et al.*, *Phys. Rev. Lett.*, **76** (1996) 3598.

- [13] N. PAPANICOLAOU and P. SPATHIS, *J. Phys.: Cond. Matt.*, **1** (1989) 5555.
- [14] J. DORIGNAC *et al.*, *Phys. Rev. Lett.*, **93** (2004) 25504.
- [15] H. MAO and R.J. HEMLEY, *Rev. Mod. Phys.*, **66** (1994) 671.